Dissociation mechanisms of the Ar trimer induced by a third atom in high-energy electron-impact ionization

S. Yan,[1] P. Zhang,[1] X. Ma,[1,*] S. Xu,[1] S. X. Tian,[2] B. Li,[1] X. L. Zhu,[1] W. T. Feng,[1] and D. M. Zhao[1]

[1]*Institute of Modern Physics, Chinese Academy of Sciences, Lanzhou 730000, China*

[2]*Hefei National Laboratory for Physical Sciences at the Microscale and Department of Chemical Physics,*
University of Science and Technology of China, Hefei, Anhui 230026, China

We experimentally studied the dissociation dynamics of a highly charged Ar_3 cluster initiated by a high-energy electron. The dissociation patterns of the correlated ions from a two-body and a three-body Coulombic explosion (CE) of $(Ar_3)^{2+}$ suggest that predissociation alters the evolution of radiative charge transfer. The three-body CE in $(Ar_3)^{4+}$ and $(Ar_3)^{5+}$ is driven, after double ionization of one constituent Ar atom, by single ionization with a simultaneous interatomic Coulombic decay process.

PACS number(s): 34.80.Gs, 34.70.+e, 36.40.−c, 82.33.Fg

The dissociation of clusters and molecules following multiple ionization can result in bond breaking and Coulombic explosion (CE). The information from CE can be used directly to map the ground-state wave function and, meanwhile, to provide a detailed understanding of chemical bond formation or breaking. The environmental enhancement effect due to the existence of neighboring atoms [1–16] is of particular importance in atmosphere science, astrophysics, and biophysics studies, which is, for example, one effective low-energy electron source inducing the damage of DNA [17]. Rare-gas clusters, characterized by a large internuclear distance and a relatively simple electronic structure, are excellent candidates for the careful examination of structural effects on the mechanisms involved in multiple-ionization dissociative decay.

In the past decades, great effort has been put into the understanding of the dissociative dynamics of linear diatomic clusters, and several environmental enhancement effects have been discovered by different experiments, such as interatomic Coulombic decay (ICD) [4–9], electron-transfer-mediated decay (ETMD) [10–12], and radiative charge transfer (RCT) [13–16]. All of the previous experimental studies have shown that the distribution of the kinetic energy release (KER), which is the sum of the kinetic energies of all fragment ions, is a good observable to distinguish the mechanisms.

However, the vast majority of rare-gas clusters are nonlinear and polyatomic. They are characterized by bonds with different bond lengths and stereo structures. When ionized, more than two atoms in a cluster are involved in the dissociative reaction. Therefore, such systems offer much richer dynamics and provide a good opportunity to discover how the structure affects the dissociation dynamics, for which the charged complex cluster may present a significant difference in the fragmentation mechanism from that of a dimer.

The Ar_3 cluster is a relatively simple yet rich example. Its predominant structure is an equilateral triangle with an average internuclear distance of 3.91 Å and bond angle of 120°. It is expected that interesting mechanisms may appear in the ionization dissociation of Ar_3, in comparison to that of Ar_2. Indeed, by simultaneously measuring the energy of the ICD electron and the KER among the three Ar^+ ions,

the sequential interatomic decay, for which the first step is an Auger decay with interatomic character and the second step is an ICD, is identified in Ar trimers in the x-ray experiment [18]. Nevertheless, the detailed ionization mechanism in the first step remains a puzzling question. The process on which we focus in this paper may shed light on this question, and furthermore, the influence of the third atom on the decay dynamics compared to the decay of an Ar dimer.

In this paper, we report an experiment that emphasizes the detailed dissociative mechanism in a highly charged argon trimer induced by a high-energy electron. The two-body and three-body CE are studied through multiple coincidence of the fragments. In contrast to the case of Ar_2, it is demonstrated that rich decay pathways have been observed in Ar_3, such as the predissociation after RCT in the two-body CE of $(Ar_3)^{2+}$ and the neutral argon atom loss after ICD. Moreover, for the three-body CE in highly charged argon trimers, $(Ar_3)^{4+}$ and $(Ar_3)^{5+}$, a mechanism is proposed as single ionization with a simultaneous ICD process.

The experiment was carried out on a reaction microscope at the Institute of Modern Physics CAS, Lanzhou [19,20]. Briefly, the pulsed electron beam with a kinetic energy of 3 keV and a pulse width of 40 ns at a 50-kHz repetition rate was used. The pulsed electron beam collides with the argon clusters, which are produced by expanding Ar gas with a 2-bars stagnation pressure through a nozzle ($\phi = 30\ \mu$m). A fraction of about 1% of dimers and even a smaller fraction of trimers and larger clusters are contained in the jet. After ionization of the Ar cluster, CE of the parent ions will be evoked through the energy- and charge-transfer processes. The recoil and fragment ions induced from CE are extracted and accelerated toward the recoil ion detector using the electrostatic field of 83.5 V/cm. The corresponding flight time (TOF) and position information are stored in event-by-event mode. The residual beam is collected into a Faraday cup.

Figure 1 shows the double-ion coincidence map resulting from the fragmentation of the Ar_n^{m+} ions produced by 3k-eV electron impact. Where n and m refer to the size and the charge state of the parent ions, T_1 and T_2 refer to the TOF of the first and the second ions, respectively. The map is characterized by bright islands (consisting of high-intensity straight lines and surrounding low-intensity "background"), vertical and horizontal straight lines, and oblique strips. The

---
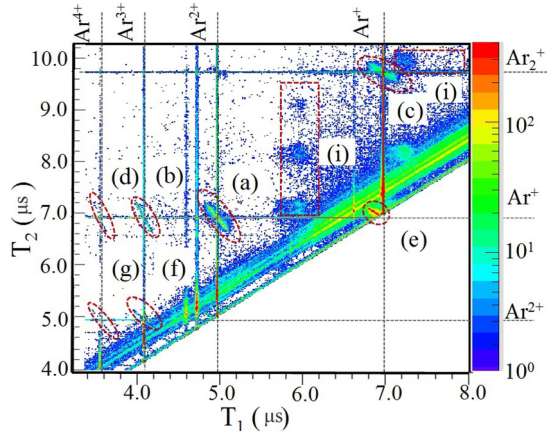
*Corresponding author: x.ma@impcas.ac.cn

FIG. 1. (Color online) Double-ion coincidence map resulting from the fragmentation of the $Ar_n{}^{m+}$ ions produced in 3000-eV electron collisions with the Ar_n clusters. T_1 and T_2 refer to the TOF of the first and second ions, respectively. The islands marked with red dashed circles (a)–(g) correspond to $Ar^{2+} + Ar^+$, $Ar^{3+} + Ar^+$, $Ar_2^+ + Ar^+$, $Ar^+ + Ar^{3+}$, $Ar^+ + Ar^+$, $Ar^{3+} + Ar^{2+}$, and $Ar^{4+} + Ar^{2+}$ ion pairs, respectively. The red rectangular region (i) depicts the ion pairs from fragmentations of the residual gas in the vacuum.

islands marked with red dashed circles, labeled with (a)–(g), are attributed to the dissociation processes of different highly charged parent ions. The slope and shape of the islands are important criteria to explore the dissociation mechanisms [21–23]. The diagonal that separates the lower right area from the upper left area is caused by the boundary condition of $T_2 = T_1 + \Delta T_d$, where ΔT_d is the dead time of the electronics for detecting a pair of ions. The oblique strip parallel to the oblique line arises from the reflection of the electron gun pulse. The horizontal and vertical lines on the map come from random coincidences between the background signals and the ions produced from the pure ionization of atoms. The rectangular area (i) is from the collisions with residual gas in the chamber, whose intensity is proportional to the quality of vacuum.

It is known that, for a two-body CE process, the two TOFs of the pair ions should be correlated. Considering that the momentum sum of the two ions must be zero, the slope of the events in the double-TOFs map should be a constant $k = -q_1/q_2$, where $q_{1,2}$ are the charge states of the two fragment ions. Indeed, the slopes of the high-intensity straight lines in the islands (a)–(g) of Fig. 1 are equal to the k values extracted from corresponding q_1 and q_2.

However, for a three-body CE, momentum conservation law is imposed on three ions, and consequently, the TOF coincidence map of the first two detected ions from a three-body CE should show a broader distribution than that from a two-body CE. The "backgrounds" in areas (a) and (b) of Fig. 1 represent these dissociation channels. To highlight the contribution of the three-body CE processes, we add a further filter condition: The third ion should be detected. The corresponding double-ion correlation map of the first and second ions is presented in Fig. 2, where the "background" in areas (a)–(c) become more pronounced than that in Fig. 1. The events in areas (a) and (b) in Fig. 2 are now attributed to the processes: $Ar_3^{4+} \rightarrow Ar^{2+} + Ar^+ + Ar^+$ and $Ar_3^{5+} \rightarrow Ar^{3+} + Ar^+ + Ar^+$, respectively.
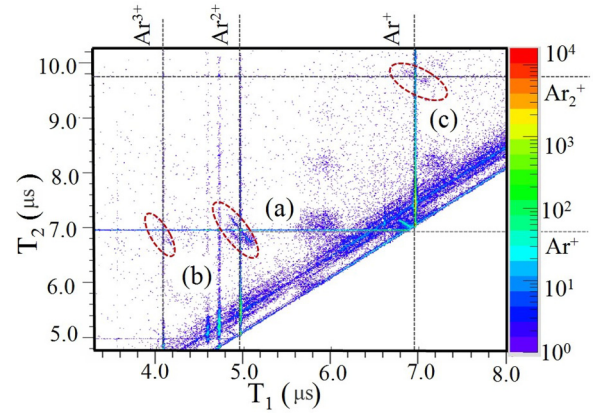

FIG. 2. (Color online) Double-ion correlation map in triple-ion coincidence of the fragmentation of the $Ar_n{}^{m+}$ ions produced in 3000-eV electron impact on Ar_n clusters. The TOF of the third detected ion is not shown. The islands marked with red dashed circles (a)–(c) correspond to $Ar^{2+} + Ar^+$, $Ar^{3+} + Ar^+$, and $Ar^+ + Ar_2^+$ ions from a three-body CE of highly charged Ar_n.

Now we focus on the two-body CE of $(Ar_3)^{2+}$, and its KER distribution of $Ar_2^+ + Ar^+$ is shown in Fig. 3. Here, only one pronounced peak located at 3.5 eV is observed, which corresponds to the CE that occurs at an internuclear distance of 3.96 Å, which coincides with the equilibrium internuclear distance of the Ar trimer [24]. This result indicates that the CE process happens so quickly that the motion of the nuclei can be ignored. It is suggested that the potential well at the distance between Ar and one Ar^+ is deep enough to bind an $(Ar_2)^+$.

It will be interesting to compare the KER distributions of two-body CEs resulting from Ar_2 and Ar_3; one may find an influence on the decay dynamics due to the existence of an additional neutral atom. It has been demonstrated that, in the KER distribution of $Ar^+ + Ar^+$ from Ar_2, the contribution of RCT is important and approximately equals that of the ICD and sequential ionization processes [19]. However, the peak
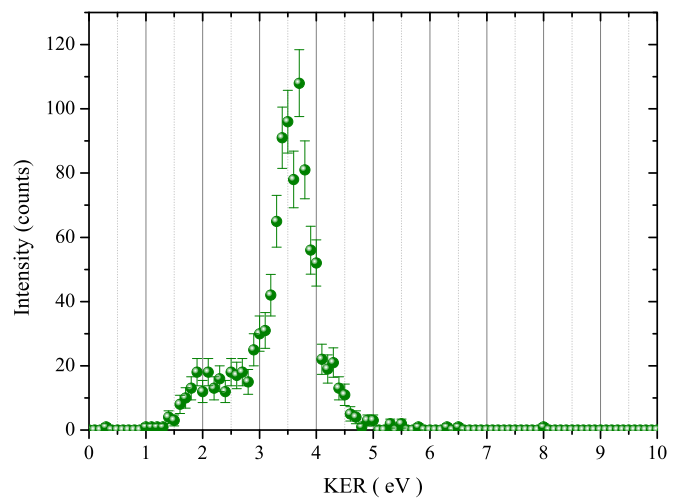

FIG. 3. (Color online) KER distribution for Ar_2^+-Ar^+ ion pairs from the fragmentation of $(Ar_3)^{2+}$.
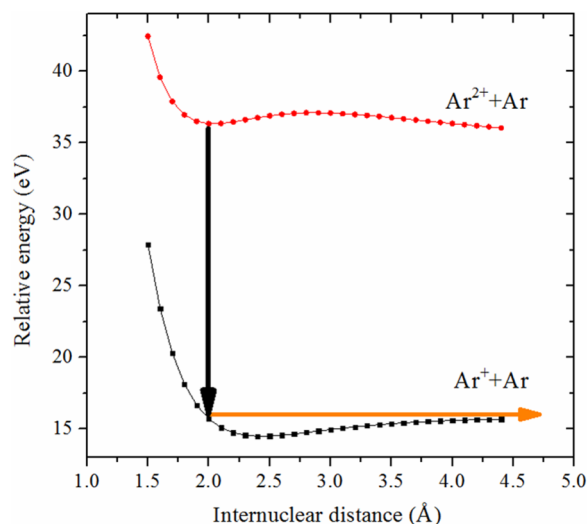
FIG. 4. (Color online) Potential energy curves from the coupled cluster method (CCSD) calculation; upper curve: the ground state of the Ar^{2+}-Ar ion, lower curve: the Ar^+-Ar ion.

FIG. 5. (Color online) KER distribution for $Ar^{2+} + Ar^+ + Ar^+$ ions from the fragmentation of $(Ar_3)^{4+}$.

corresponding to the RCT process, which should locate in the larger energy area, does not appear at all in Fig. 3. What is the origin of the present scenario for Ar_3?

According to theoretical calculations, the structural evolution of a charged Ar trimer completes in 1 ps after single ionization, and it transfers from the most stable equilateral triangle of Ar_3 to the linear-symmetric structure of the Ar_3^+ ion because of the directional character of the empty p orbital [25–27]. Despite the fact that the cluster ion in our case is Ar_3^{2+} instead of Ar_3^+, the assumption of the linear-symmetric structure for the Ar_3^{2+} ion should be reasonable, e.g., an Ar^{2+} ion initially produced by $(e, 3e)$ ionization locates in the center of the Ar_3 ion with the two neutral atoms on either side. The equilibrium internuclear distance (EID) between the Ar^{2+} and each Ar atom will be similar to that of the $(Ar_2)^{2+}$ ion. For the Ar-Ar^{2+}-Ar initial state, the charge transfer can also happen during the vibration, similar to what occurred in the $(Ar_2)^{2+}$ ion; e.g., one valence electron from one neutral atom will be transferred to the Ar^{2+} ion near its EID through the RCT process. However, because the EID of Ar^{2+}-Ar is much shorter than that of Ar^+-Ar (see Fig. 4), the sudden change of charge state at a closer internuclear distance make the Ar^+-Ar ion populate in a predissociation state, resulting in the loss of the neutral Ar atom. Consequently, the predissociation terminates the evolution of RCT, and leads to three-body fragmentation $(Ar^+ + Ar^+ + Ar)$ instead of an $Ar^+ + Ar_2^+$ RCT peak.

As previously pointed out, the information of a three-body CE could be extracted from the triple-coincidence map of Fig. 2. The KER distribution of $Ar^{2+} + Ar^+ + Ar^+$ ions presented in Fig. 5 are from a three-body CE, $Ar_3^{4+} \rightarrow Ar^{2+} + Ar^+ + Ar^+$ [area (a) of Fig. 2], in which only one peak at 17.5 eV is observed. The average bond length estimated is approximately 3.96 Å, which is consistent with the EID (3.91 Å) from the triangle structure of the Ar_3 [24]. This finding reveals that the simultaneous breakup of all bonds occurs in the equilateral triangle structure of the Ar trimer and that the breakup is so swift that there is little time remaining for
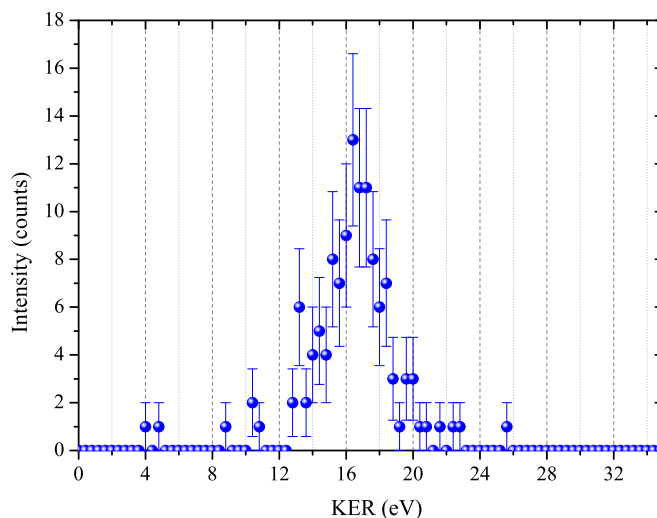
nuclear motion. In contrast, the contribution of mechanisms involving the RCT process, which should locate in a larger KER energy area, is negligible.

How are we to figure out the origin and decay of $(Ar_3)^{4+}$? The study of fragmentation of a triply ionized Ar dimer [19] has shown that the neighboring Ar atom can be ionized by the decay of the excited Ar^{2+*} state via the ICD process, and then, the ion pair $Ar^{2+} + Ar^+$ is followed by a two-body CE process. In the case of an Ar trimer, initial $(e, 3e)$ ionization produces an intermediate state $(Ar$-Ar^{2+*}-$Ar)$. One neutral atom can also be ionized through ICD, provided that the Ar^{2+} populate the excited state and the excess energy is insufficient to ionize one of its own valence electrons. Then the intermediate cluster ion Ar^{2+*}-Ar^+-Ar is formed. The other neutral Ar atom in the cluster ion may have the following four pathways to achieve its final stable state. First, it may be bound by the ion Ar^+ and form the cluster ion Ar^{2+}-Ar_2^+. Then, due to the repulsive Coulombic force, the two ions will depart from each other quickly and will finally result in an $Ar^{2+} + Ar_2^+$ ion pair; second, the Ar atom may also be caught by the Ar^{2+} ion and form an $(Ar_2)^{2+}$ ion. In this case, the transition is a vertical process and the $(Ar_2)^{2+}$ ion will be populated in a high vibrational state. As the two nuclei approach, the RCT process occurs and leads the cluster ion $(Ar_2)^{2+}$ into the Ar^+-Ar^+ state. Consequently, the parent ion produces $Ar^+ + Ar^+ + Ar^+$ by CE.

Third, the neutral atom Ar can be ionized by the outgoing electrons from the initial $(e, 3e)$ reaction. Because the time scales of single ionization and ICD are less than or on the order of a few femtoseconds, the Ar_3^{4+} will break via CE at the equilibrium distance of the Ar_3. Indeed, the observed KER peak at 17.5 eV of the $Ar^{2+} + Ar^+ + Ar^+$ ions confirms this assumption, which indicates the important role of secondary ionization by the emitted electrons in the fragmentation of a highly charged Ar trimer.

Fourth, sequential ICD also seems to be a possible pathway: A highly excited Ar^{2+} ion produced in the first step results in the first ICD, but this mechanism requires that a highly

excited Ar^+ ion should be formed. Then, the second ICD between the excited Ar^+ ion and another Ar atom ionizes its one outer-shell electron. As a result, the three-body CE among the $Ar^{2+} + Ar^+ + Ar^+$ ions will occur at the EID of the Ar_3. However, to obtain an excited Ar^+ ion requires a $2p$ inner-shell ionization; the corresponding binding energy is 245 eV. It is much larger than the triple-ionization energy of Ar (85 eV), which means that the prerequisite condition of sequential ICD is not satisfied.

Now, let us examine the two-dimensional map in Fig. 1. The interesting area of the two-body CE of Ar^{2+}-Ar_2^+ has a very weak intensity, which indicates that most of the Ar_2^+ ions formed in highly charged Ar_3 are unstable. On the other hand, if a RCT process occurred as in mechanism (2), the corresponding KER peak should locate at a larger energy position than that of the CE from the equilibrium internuclear distance [19]. However, most of the detected Ar^+ ions in triple coincidence are from the ICD following Auger decay, like that determined in x-ray experiments [18]. Therefore, the contributions related to mechanisms (1) and (2) are negligible. This phenomenon indicates that the Coulomb repelling force of the two ions Ar^+ and Ar^{2+} is larger than the polarization attracting force between Ar and Ar^{2+} and the formation of an $(Ar_2)^+$ or $(Ar_2)^{2+}$ ion is not possible, which demonstrates that the neutral atom can be lost easily if more than one ion is highly charged in the Ar_3 cluster. Therefore, in pathway (3), one neighboring atom is ionized by the emitted electrons, while the third atom is ionized through ICD due to the deexcitation of the first doubly ionized argon atom. This is the dominant process, which is termed single ionization with a simultaneous ICD (SI-ICD).

Furthermore, we would like to address the formation and decay of Ar_3^{5+} through complete Coulomb explosion into three Ar ions. Similar analysis demonstrates that initial triple ionization forms an intermediate state (Ar-Ar^{3+*}-Ar), and one neighboring atom is ionized by the outgoing electrons, while the third atom is ionized through ICD due to the deexcitation of the first ionized argon atom. Indeed, the similarity can be found in Fig. 2 for a three-body CE indicated by areas (a) and (b). This phenomenon indicates that the formation of $Ar^{3+} + Ar^+ + Ar^+$ ions also arises from SI-ICD.

In conclusion, electron-impact ionization of an Ar trimer reveals the rich dynamics induced by an additional neutral atom in it. By comparing the KER distribution of fragments from the $(Ar_3)^{2+}$ with that from $(Ar_2)^{2+}$, and on the basis of the accurate potential energy curves of $(Ar_2)^+$ and $(Ar_2)^{2+}$, it is found that ICD and sequential ionization are by far the dominant mechanisms while the predissociation terminates RCT in the fragmentation of $(Ar_3)^{2+}$. The two-body CE and three-body CE of the Ar_3 ions demonstrate that the neutral atom in the highly charged Ar_3 ion can be lost easily and affects decay dynamics efficiently. The present studies indicate that, after double and triple ionization of one constituent Ar atom, the dominant mechanism driving three-body CE of $(Ar_3)^{4+}$ and $(Ar_3)^{5+}$ is single ionization with a simultaneous ICD process.

[1] R. Santra, J. Zobeley, and L. S. Cederbaum, Phys. Rev. B **64**, 245104 (2001).

[2] B. Ulrich, A. Vredenborg, A. Malakzadeh, L. Ph. H. Schmidt, T. Havermeier, M. Meckel, K. Cole, M. Smolarski, Z. Chang, T. Jahnke, and R. Dörner, J. Phys. Chem. A **115**, 6936 (2011).

[3] T. Pflüger, http://archiv.ub.uni-heidelberg.de/volltextserver/13325/.

[4] L. S. Cederbaum, J. Zobeley, and F. Tarantelli, Phys. Rev. Lett. **79**, 4778 (1997).

[5] S. Marburger, O. Kugeler, U. Hergenhahn, and T. Moller, Phys. Rev. Lett. **90**, 203401 (2003).

[6] T. Jahnke, A. Czasch, M. S. Schöffler, S. Schössler, A. Knapp, M. Käsz, J. Titze, C. Wimmer, K. Kreidi, R. E. Grisenti, A. Staudte, O. Jagutzki, U. Hergenhahn, H. Schmidt-Böcking, and R. Dörner, Phys. Rev. Lett. **93**, 163401 (2004).

[7] T. Aoto, K. Ito, Y. Hikosaka, E. Shigemasa, F. Penent, and P. Lablanquie, Phys. Rev. Lett. **97**, 243401 (2006).

[8] Y. Morishita, X.-J. Liu, N. Saito, T. Lischke, M. Kato, G. Prümper, M. Oura, H. Yamaoka, Y. Tamenori, I. H. Suzuki, and K. Ueda, Phys. Rev. Lett. **96**, 243402 (2006).

[9] R. Santra and L. S. Cederbaum, Phys. Rev. Lett. **90**, 153401 (2003).

[10] J. Zobeley, R. Santra, and L. S. Cederbaum, J. Chem. Phys. **115**, 5076 (2001).

[11] K. Sakai, S. Stoychev, T. Ouchi, I. Higuchi, M. Schöffler, T. Mazza, H. Fukuzawa, K. Nagaya, M. Yao, Y. Tamenori, A. I. Kuleff, N. Saito, and K. Ueda, Phys. Rev. Lett. **106**, 033401 (2011).

[12] M. Förstel, M. Mucke, T. Arion, A. M. Bradshaw, and U. Hergenhahn, Phys. Rev. Lett. **106**, 033402 (2011).

[13] R. Johnsen and M. A. Biondi, Phys. Rev. A **18**, 996 (1978).

[14] N. Saito, Y. Morishita, I. H. Suzuki, S. D. Stoychev, A. I. Kuleff, L. S. Cederbaum, X.-J. Liu, H. Fukuzawa, G. Prümper, and K. Ueda, Chem. Phys. Lett. **441**, 16 (2007).

[15] J. Matsumoto, A. Leredde, X. Flechard, K. Hayakawa, H. Shiromaru, J. Rangama, C. L. Zhou, S. Guillous, D. Hennecart, T. Muranaka, A. Mery, B. Gervais, and A. Cassimi, Phys. Rev. Lett. **105**, 263202 (2010).

[16] B. Ulrich, A. Vredenborg, A. Malakzadeh, M. Meckel, K. Cole, M. Smolarski, Z. Chang, T. Jahnke, and R. Dörner, Phys. Rev. A **82**, 013412 (2010); B. Manschwetus, H. Rottke, G. Steinmeyer, L. Foucar, A. Czasch, H. Schmidt-Böcking, and W. Sandner, ibid. **82**, 013413 (2010).

[17] B. Boudaiffa, P. Cloutier, D. Hunting, M. A. Huels, and L. Sanche, Science **287**, 1658 (2000); G. Hanel, B. Gstir, S. Denifl, P. Scheier, M. Probst, B. Farizon, M. Farizon, E. Illenberger, and T. D. Märk, Phys. Rev. Lett. **90**, 188104 (2003).

[18] X. Liu, N. Saito, H. Fukuzawa, Y. Morishita, S. Stoychev, A. Kuleff, I. H. Suzuki, Y. Tamenori, R. Richter, G. Prümper, and K. Ueda, J. Phys. B: At. Mol. Opt. Phys. **40**, F1 (2007).

[19] S. Yan, P. Zhang, X. Ma, S. Xu, B. Li, X. L. Zhu, W. T. Feng, S. F. Zhang, D. M. Zhao, R. T. Zhang, D. L. Guo, and H. P. Liu, Phys. Rev. A **88**, 042712 (2013).

[20] J. Ullrich, R. Moshammer, A. Dorn, R. Dörner, L. Ph. H. Schmidt, and H. Schmidt-Böcking, Rep. Prog. Phys. **66**, 1463 (2003).

[21] J. H. D. Eland, Mol. Phys. **61**, 725 (1987).

[22] J. H. D. Eland, Laser Chem. **11**, 259 (1991).

[23] E. Ruhl, C. Heinzel, H. Baumgärtel, M. Lavollée, and P. Morin, Z. Phys. D **31**, 245 (1994); E. Ruhl, Int. J. Mass Spectrom. **229**, 117 (2003).

[24] S. Rick, D. L. Lynch, and J. D. Doll, J. Chem. Phys. **95**, 3506 (1991).

[25] J. Galindez, F. Calvo, P. Paska, D. Hrivnak, R. Kalus, and F. X. Gadéa, Comput. Phys. Commun. **145**, 126 (2002).

[26] W. R. Wadt, Appl. Phys. Lett. **38**, 1030 (1981).

[27] H. Haberland, B. von Issendorff, T. Kolar, H. Kornmeier, C. Ludewigt, and A. Risch, Phys. Rev. Lett. **67**, 3290 (1991).